

UC Irvine

UC Irvine Previously Published Works

Title

Phosphorylation at Serine 21 in G protein-coupled receptor kinase 1 (GRK1) is required for normal kinetics of dark adaption in rod but not cone photoreceptors.

Permalink

<https://escholarship.org/uc/item/7c86x8rw>

Journal

The FASEB Journal, 34(2)

Authors

Kolesnikov, Alexander

Chrispell, Jared

Osawa, Shoji

et al.

Publication Date

2020-02-01

DOI

10.1096/fj.201902535R

Peer reviewed



Published in final edited form as:

FASEB J. 2020 February ; 34(2): 2677–2690. doi:10.1096/fj.201902535R.

Phosphorylation at Serine 21 in G protein-coupled receptor kinase 1 (GRK1) is required for normal kinetics of dark adaptation in rod but not cone photoreceptors

Alexander V. Kolesnikov¹, Jared D. Chrispell², Shoji Osawa², Vladimir J. Kefalov¹, Ellen R. Weiss²

¹Department of Ophthalmology and Visual Sciences, Washington University School of Medicine, Saint Louis, MO, USA

²Department of Cell Biology and Physiology, The University of North Carolina, Lineberger Comprehensive Cancer Center, Chapel Hill, NC, USA

Abstract

Timely recovery of the light response in photoreceptors requires efficient inactivation of photoactivated rhodopsin. This process is initiated by phosphorylation of its carboxyl terminus by G protein-coupled receptor kinase 1 (GRK1). Previously, we showed that GRK1 is phosphorylated in the dark at Ser21 in a cAMP-dependent manner and dephosphorylated in the light. Results in vitro indicate that dephosphorylation of Ser21 increases GRK1 activity, leading to increased phosphorylation of rhodopsin. This creates the possibility of light-dependent regulation of GRK1 activity and its efficiency in inactivating the visual pigment. To address the functional role of GRK1 phosphorylation in rods and cones in vivo, we generated mutant mice in which Ser21 is substituted with alanine (GRK1-S21A), preventing dark-dependent phosphorylation of GRK1. GRK1-S21A mice had normal retinal morphology, without evidence of degeneration. The function of dark-adapted GRK1-S21A rods and cones was also unaffected, as demonstrated by the normal amplitude and kinetics of their responses obtained by ex vivo and in vivo ERG recordings. In contrast, rod dark adaptation following exposure to bright bleaching light was significantly delayed in GRK1-S21A mice, suggesting that the higher activity of this kinase results in enhanced rhodopsin phosphorylation and therefore delays its regeneration. In contrast, dark adaptation of cones was unaffected by the S21A mutation. Taken together, these data suggest that rhodopsin phosphorylation/dephosphorylation modulates the recovery of rhodopsin to the ground state and

Correspondence Vladimir J. Kefalov, Department of Ophthalmology & Visual Sciences, Washington University School of Medicine, 660 S. Euclid Avenue, Campus Box 8096, Saint Louis, MO 63110, USA, kefalov@wustl.edu; Ellen R. Weiss, Department of Cell Biology & Physiology, The University of North Carolina, CB# 7545, 5340B MBRB, 111, Mason Farm Rd., Chapel Hill, NC 27599-7090, USA. erweiss@med.unc.edu.

AUTHOR CONTRIBUTIONS

A. V. Kolesnikov designed and performed experiments, analyzed and interpreted data and helped to draft and finalize the manuscript; J.D. Chrispell designed and performed experiments, analyzed and interpreted data and helped revise the manuscript; S. Osawa designed and performed experiments, analyzed and interpreted data. V.J. Kefalov designed experiments, interpreted data, and helped to draft and finalize the manuscript; E.R. Weiss designed experiments, interpreted data and helped to draft and finalize the manuscript. All authors approved the final version of the manuscript.

CONFLICT OF INTEREST

The authors declare no conflicts of interest with the contents of this article.

rod dark adaptation. They also reveal a novel role for cAMP-dependent phosphorylation of GRK1 in regulating the dark adaptation of rod but not cone photoreceptors.

Keywords

cAMP; photoreceptor; phototransduction; protein phosphorylation; vision

1 | INTRODUCTION

Rhodopsin activation in vertebrate rod photoreceptors triggers a canonical G protein-coupled receptor (GPCR) signaling cascade similar to that of most other GPCRs. Activation by a single photon of light induces a conformational change in rhodopsin that allows it to activate its G protein, transducin, which, in turn, activates PDE6, a phosphodiesterase that hydrolyzes cGMP, thereby shutting down cGMP-gated cation channels in the rod cell membrane.^{1,2} Light-activated rhodopsin is also a substrate for GRK1, a G protein-coupled receptor kinase found in all vertebrate rods examined to date, with the exception of snakes, and in many vertebrate cones³⁻⁷ (for review, see Ref. 8). Phosphorylation of visual pigment by GRK1 partially blocks its activity and induces the binding of arrestin, which completely blocks the pigment interaction with transducin and prevents downstream signaling.^{9,10} The phosphorylation of rhodopsin and cone opsin by GRK1 is modulated by recoverin, a calcium-binding protein that suppresses the phosphorylation of the pigment by GRK1 in high calcium, thus prolonging its activity and increasing the sensitivity of photoreceptors to dim light.^{11,12}

Dark adaptation is typically defined as the ability to regain photosensitivity after bright light stimulation, which, in the case of rods, is very slow, requiring 1-3 hours.^{13,14} In both rods and cones, dark adaptation requires regeneration of the bleached visual pigment, a process that involves the dephosphorylation of the opsins, the release of all-*trans*-retinal from the pigment, and the binding of fresh 11-*cis*-retinal following its recycling.¹⁵⁻¹⁷ Recently, it has been shown that both rhodopsin and the M-cone pigment are dephosphorylated by protein phosphatase 2A (PP2A), allowing them to reset to their ground state in a timely fashion and respond to another photon.¹⁸

To allow photoreceptors to revert to their dark-adapted state after exposure to bright bleaching light, additional factors may also modulate the lifetime and recovery of the visual pigment after photoactivation. We previously determined that Ser21 in GRK1 and Ser36 in GRK7 (a cone opsin kinase; Refs. 3, 19, 20) are cAMP-dependent phosphorylation sites.²¹ Photoreceptor cAMP levels are high in the dark and low in the light.^{22,23} Phosphorylation of GRK1 and GRK7 at these residues was also high in the dark and low in the light in vivo,^{24,25} with light-mediated dephosphorylation of GRK1 occurring independent of phototransduction.²⁵ Biochemical studies have shown that phosphorylation at the amino-terminus by cAMP-dependent protein kinase (PKA) decreases the activity of these GRKs, making them less effective at phosphorylating rhodopsin.²¹ Thus, the efficiency of rhodopsin inactivation and regeneration could potentially be modulated by the dark/light- and cAMP-dependent phosphorylation of GRK1. Although no biochemical studies have been performed

with cone opsins so far, a similar GRK1-dependent regulation could potentially exist in mammalian cones, including in species whose cones lack GRK7, such as rat and mouse.²⁶ In the present report, we have used a genetically engineered GRK1-S21A mouse in which the amino acid Ser21, the cAMP-dependent phosphorylation site in GRK1 in vivo,²⁵ has been substituted by alanine. We used these mice to determine the role of GRK1 phosphorylation at Ser21 in modulating the function of rod and cone photoreceptors. Our results demonstrate that the S21A substitution in GRK1 does not affect phototransduction in dark-adapted mouse rods and cones in response to dim or saturating flashes. However, the ability of GRK1-S21A rods to dark-adapt following a nearly complete pigment bleach was markedly suppressed, suggesting that phosphorylation of GRK1 at Ser21 helps to modulate the resetting of rhodopsin to its ground state and the dark adaptation of rods. In contrast, cone dark adaptation was normal in mutant mice indicating the lack of a regulatory effect of GRK1 phosphorylation on cone opsin regeneration.

2 | MATERIALS AND METHODS

2.1 | Antibodies

A polyclonal antibody (anti-pGRK1), that specifically recognizes phosphorylation of GRK1 at Ser21, was generated by 21st Century Biochemicals (Marlboro, MA).²⁵ A monoclonal antibody (D11) that recognizes GRK1 was purchased from Affinity Bioreagents (Rockford, IL). A rabbit polyclonal antibody against holo-transducin (G_t) was a gift from Dr. Gary L. Johnson (The University of North Carolina at Chapel Hill, NC). A monoclonal anti-actin antibody was purchased from MilliporeSigma (St. Louis, MO). Secondary antibodies AlexaFluor goat anti-rabbit IgG and IRDy3800 goat anti-mouse IgG were purchased from ThermoFisher (Waltham, MA).

2.2 | Mice

C57Bl6/J, B6.C-Tg(CMV-cre)1Cgn/J, and C57BL/6N-PRX-B6N mice were obtained from Jackson Laboratories (Bar Harbor, ME). The *Grk1*^{-/-} mice were a gift from Dr Ching-Kang Chen (Baylor College of Medicine). The generation of the GRK1-Ser21A knock-in mice is described in the Results section. For all cone physiological experiments, GRK1-S21A-*Gnat1*^{-/-} animals and their littermate GRK1-WT-*Gnat1*^{-/-} controls were generated by crossing GRK1-S21A mice with the rod transducin α -subunit knockout (*Gnat1*^{-/-}) mouse line lacking rod phototransduction.²⁷

2.3 | Western blot and outer nuclear layer thickness analysis

For western blot analysis, wild-type C56Bl/6J, *Grk1*^{-/-}, and GRK1-S21A mice raised in cyclic light were dark-adapted overnight. Then mice were either exposed to 1500 lux of white light for 1 hour or maintained in the dark. Mice were euthanized in the light or in the dark by cervical dislocation and the eyes enucleated for removal of the retinas. The eyes were placed in HEPES-Ringer buffer consisting of 10 mM HEPES, pH 7.5, 120 mM sodium chloride, 0.5 mM potassium chloride, 0.2 mM calcium chloride, 0.2 mM magnesium chloride, 0.1 mM EDTA, 10 mM glucose, and 1 mM DTT.^{25,28} Retinas from light exposed mice were removed from eye cups in the light using a conventional dissection microscope. Alternatively, retinas from mice maintained in the dark were removed under dim red light

using an infrared dissection microscope.²⁵ For homogenization, each retina was placed in 100 μ L of HEPES-Ringer buffer, followed by the addition of 150 μ L of buffer consisting of 125 mM Tris-HCl, pH 6.8, 5% SDS, 20% glycerol, and 100 mM NaF preheated to 95°C. The mixture was homogenized for 20 s with a motorized pestle, heated for 3 minutes at 95°C, then sheared with a 25-gauge needle. After centrifugation at 10 000g for 10 minutes at 25°C to remove insoluble material, the supernatant was collected for protein determination and analyzed by SDS-PAGE. Each lane contained 25 μ g of retinal lysate. For western blot analysis, the gel was transferred to nitrocellulose and the membrane incubated for 1 hour in Odyssey Blocking Buffer (Licor Biosciences, Lincoln, NE), then incubated overnight at 4°C with the following primary antibodies: anti-pGRK1 (1:1000), anti-GRK1 (1:10 000), anti-actin, (1:5000), and anti-transducin (1:2500). Secondary antibodies IRDye800 (goat anti-mouse IgG) and AlexaFluor 680 (goat anti-rabbit IgG) were both used at 1:10 000.

For quantitative analysis of the outer nuclear layer (ONL) thickness, wild-type and GRK1-S21A mice were euthanized with 100 mg/kg ketamine. The chest was dissected to expose the heart and the mouse was perfused with 4% paraformaldehyde followed by cervical dislocation. Eyes were enucleated and placed in a solution of 2% glutaraldehyde, 2% paraformaldehyde, 50 mM MOPS and 0.05% CaCl₂ (w/v), pH 7.2 overnight. The eyes were transferred to PBS, then incubated in 2% osmium tetroxide in 0.1% cacodylate buffer (0.1 M, pH 7.3) for 90 minutes at room temperature. After rinsing twice in cacodylate buffer for 15 minutes, the eye cups were dehydrated through a series of ethanol concentrations for 15 minutes at each concentration (50%, 70%, 80%, 90%, 95%, and twice in 100% ethanol). Dehydration was followed by two 15-min incubations in propylene oxide. Eye cups were incubated overnight under vacuum in a 1:1 mixture of propylene oxide and epon812, then transferred to 100% epon812 for 6 hours at 65°C, followed by embedding overnight at 65°C under vacuum. Eye cups were sectioned at 0.5 μ m using a Leica-Reichert Ultracut microtome and stained with 1% methylene blue. Imaging of whole retina sections was performed using tile scanning and capture with a Nikon Ti2 inverted microscope (Nikon, Tokyo, Japan). The width of the ONL was measured in sections cut through the optic nerve at 500- μ m steps from the optic nerve head (ONH) using Image J.²⁹ For statistical analysis, multiple unpaired *t* tests with Holm-Sidak's comparison correction were performed using GraphPad Prism (La Jolla, CA).

2.4 | Ex vivo rod recordings from isolated mouse retinas

Mice were dark-adapted overnight and sacrificed by CO₂ asphyxiation. The whole retina was removed from each mouse eyecup under infrared illumination and stored in oxygenated aqueous L15 (13.6 mg/mL, pH 7.4) solution (Sigma-Aldrich) containing 0.1% BSA, at room temperature. The retina was mounted on filter paper with the photoreceptor side up and placed in a perfusion chamber³⁰ between two electrodes connected to a differential amplifier. The tissue was perfused with bicarbonate-buffered Ames medium (Sigma-Aldrich) supplemented with 40 μ M DL-2-amino-4-phosphonobutyric acid to block postsynaptic components of the photoresponse,³¹ and with 100 μ M BaCl₂ to suppress the slow glial PIII component.³² The perfusion solution was continuously bubbled with a 95% O₂/5% CO₂ mixture and heated to 36-37°C.

The photoreceptors in the retina were stimulated with 20-ms test flashes of calibrated 505 nm LED light. The light intensity was controlled by a computer in 0.5 log unit steps. Intensity-response relationships were fitted with the following Naka-Rushton hyperbolic functions:

$$R = \frac{R_{\max} \cdot I^n}{I^n + I_1^n / 2}, \text{ for raw data, or}$$

$$\frac{R}{R_{\max}} = \frac{I^n}{I^n + I_1^n / 2}, \text{ for normalized data,}$$

where R is the transient-peak amplitude of the rod or cone response, R_{\max} is the maximal response amplitude, I is the flash intensity, n is the Hill coefficient (exponent), and $I_{1/2}$ is the half-saturating light intensity. Photoresponses were amplified by a differential amplifier (DP-311, Warner Instruments), low-pass filtered at 300 Hz (8-pole Bessel), and digitized at 1 kHz. Data were analyzed with Clampfit 10.4 and Origin 8.5 software.

2.5 | In vivo electroretinography (ERG)

Dark-adapted mice were anesthetized with an intraperitoneal injection of a mixture of ketamine (100 mg/kg) and xylazine (20 mg/kg). Pupils were dilated with a drop of 1% atropine sulfate. Mouse body temperature was maintained at 37°C with a heating pad. ERG responses were measured from both eyes by contact corneal electrodes held in place by a drop of Gonak solution (Akorn). Full-field ERGs were recorded with a UTAS BigShot apparatus (LKC Technologies) using Ganzfeld-derived test flashes of calibrated green 530 nm LED light.

Rod a-wave fractional flash sensitivity (S_f) was calculated from the linear part of the intensity-response curve, as follows:

$$S_f = \frac{A}{A_{\max} \cdot I},$$

where A is the rod a-wave dim flash response amplitude, A_{\max} is the maximal response amplitude for that eye (determined at 23.5 cd•m⁻²), and I is the flash strength. Similarly, cone b-wave flash sensitivity (S_f) in control (*Gnat1*^{-/-}) and GRK1-S21A-*Gnat1*^{-/-} mice were determined after normalization of the dim flash response to the maximal b-wave amplitude obtained with the brightest white light stimulus from the Xenon Flash tube (700 cd•m⁻²). The b-wave measurements were used for all cone in vivo ERG recordings because of the very small magnitude of the cone a-wave in these conditions. The sensitivity of rods or cones was first determined in the dark. To monitor the postbleach recovery of rod ERG A_{\max} and rod S_f or cone S_f the bulk (>90%) of respective visual pigment was bleached with a 35-s exposure to 520 nm LED light focused at the surface of the cornea. The bleached fraction was estimated from the following equation:

$$F = 1 - e^{(-I \cdot P \cdot t)},$$

where F is the fraction of pigment bleached, t is the duration of the light exposure (s), I is the bleaching light intensity of 520 nm LED light (1.3×10^8 photons $\mu\text{m}^{-2} \text{s}^{-1}$), and P is the photosensitivity of mouse photoreceptors at the wavelength of peak absorbance (5.7×10^{-9} μm^2 for mouse rods³³; and 7.5×10^{-9} μm^2 for mouse cones³⁴). Mice were re-anesthetized every 30-40 minutes with a lower dose of ketamine (~1/2 of the initial dose) and a 1:1 mixture of PBS and Gonak solutions was gently applied to their eyes with a plastic syringe to protect them from drying and maintain electrode contacts.

2.5.1 | Statistics—For all experiments, data were expressed as mean \pm SEM and analyzed with the independent two-tailed Student's t test (using an accepted significance level of $P < .05$).

3 | RESULTS

3.1 | Generation of GRK1-S21A mice

GRK1-S21A knock-in mice were generated by homologous recombination in C57BL/6N ES cells. A gene targeting vector was constructed by recombineering using a BAC clone containing the full-length mouse gene for GRK1 (Figure 1A). The targeting vector included a mutation of serine 21 to alanine in exon 1 and a *loxP*-flanked PGK-Neomycin resistance cassette in intron 1 (Figure 1B). The targeting vector was electroporated into C57BL/6N-PRX-B6N ES cells and clones were screened by PCR and Southern blot analysis. The presence of the S21A mutation was confirmed in clones by PCR amplification and digestion with *SfoI*, a novel restriction enzyme site created by the mutation. Correctly targeted cells were injected into C57BL/6-albino blastocysts for chimera formation. Chimeras were mated to C57BL/6-albino animals for germline transmission of the targeted allele. Insertion of the mutant DNA into the germline was further validated by PCR screening. Positive mice were mated to a *Cre* deleter line, B6.C-Tg(CMV-cre)1Cgn/J, to remove the floxed Neocassette. Finally, the resulting line containing the S21A mutation was backcrossed to homozygosity and crossed into C57Bl/6J mice to ensure the absence of the *rd8* mutation.

3.2 | Analysis of GRK1 phosphorylation in wild-type and GRK1-S21A mice

We began our analysis by determining how the S21A mutation of GRK1 affects the expression level and phosphorylation of this enzyme. All mice were dark-adapted overnight, then either exposed to light or maintained in the dark as described in the Methods. Retinas from light-exposed or dark-adapted wild-type mice and retinas from *Grk1*^{-/-} animals were analyzed by western blot analysis using antibodies recognizing GRK1 phosphorylated at Ser21 (anti-pGRK1) or total GRK1 (D11) to determine the levels of GRK1 phosphorylation under these different conditions (Figure 2A). Phosphorylation of GRK1 was high in dark-adapted control retinas and low in light-adapted retinas, as expected. A faint band was detected in the light-adapted retinas, which we speculate could be the result of weak cross reactivity between the anti-pGRK1 antibody and GRK1, based on the absence of this band in GRK1-deficient mice (Reprinted from Ref. 25; see Figure Legend). The S21A point mutation resulted in elimination of GRK1 phosphorylation at that site in the dark (Figure 2B). Notably, the control and GRK1-S21A retinas had very similar amounts of total GRK1, indicating that the S21A mutation does not affect the expression level of GRK1 in

photoreceptors. In addition, all three subunits of rod transducin were detected at similar levels in the two mouse strains (Figure 2C). We also compared the thickness of the outer nuclear layers in the wild-type and mutant mice to determine whether the GRK1-S21A animals undergo retinal degeneration (Figure 3). No thinning of the outer nuclear layer at any retinal location was observed in 4-month-old GRK1-S21A mice compared with their age-matched controls by microscopy (Figure 3A,B) or measuring the width of the ONL (Figure 3C), except at the very superior edge of the sections. Therefore, mutating GRK1 to block its phosphorylation at Ser21 did not affect its expression or cause detectable retinal degeneration. This allowed us to perform a comprehensive physiological analysis of the GRK1-S21A mice to determine the functional role of Ser21 phosphorylation of GRK1 in mammalian rods.

3.3 | Phototransduction in rods of GRK1-S21A mice

To investigate whether the S21A mutation in GRK1 affects the phototransduction cascade in mouse rods and their physiological function, we performed transretinal ERG recordings from dark-adapted animals in the presence of synaptic blockers (Figure 4). If the lack of GRK1 phosphorylation caused by this mutation generates a highly active form of the enzyme, an increased fraction of rhodopsin may remain phosphorylated in GRK1-S21A rods, possibly even after overnight dark adaptation. As phosphorylated rhodopsin is less efficient in activating the phototransduction cascade,³⁵ this would be expected to lower its amplification and reduce the sensitivity of dark-adapted GRK1-S21A rods.

In agreement with the normal density of mutant rods and the well-preserved structure of their outer segments, retinas from dark-adapted control and GRK1-S21A mice produced saturated responses of comparable amplitudes, around 600 μ V (Figure 4A,B). The fractional dim flash responses of GRK1-S21A retinas were of essentially identical amplitude to those from controls (Figure 4C). In addition, their kinetics were also comparable, with average time-to-peak values of 131 and 132 ms, respectively (Figure 4C). Notably, both phototransduction activation, measured from the rising phase of the dim flash response, and its inactivation were unaffected by the S21A mutation in GRK1 (Figure 4C). The recovery following saturating flashes was also normal in GRK1-S21A mice, as evident from the similar shapes of their maximal responses at identical strengths of stimulating light (Figure 4D). Finally, the rod photosensitivity of mutant animals was also normal after overnight dark adaptation (Figure 4E,F).

Together, these results indicate that the presence of a highly active S21A mutant form of GRK1 in mouse rods does not affect their overall health and does not compromise their signaling under dark-adapted conditions. The normal dark-adapted sensitivity of mutant rods also indicates that their visual pigment is dephosphorylated after overnight dark adaptation, similar to wild-type rods.

3.4 | Suppressed rod dark adaptation in GRK1-S21A mice

The results above clearly demonstrate that the S21A mutation in GRK1 does not affect the function of rods under dark-adapted conditions. We next investigated, with *in vivo* ERG recordings, whether enhanced rhodopsin phosphorylation by the more active mutant GRK1

modulates the dark adaptation of mouse rods. It is well established that the dark adaptation of rods *in vivo* is generally driven by the decay of photoactivated rhodopsin and its subsequent regeneration with fresh 11-*cis*-retinal supplied by the retinal pigment epithelium (RPE) through the visual cycle. The kinetics of rod dark adaptation were measured by monitoring the recovery of rod ERG a-wave amplitude and dim flash sensitivity after exposure to bright light that nearly completely (>90%) bleached the rod pigment.

We first recorded rod-driven scotopic ERG responses in the dark and found that their waveforms and maximal amplitudes were comparable in control mice ($317 \pm 9 \mu\text{V}$, $n = 16$) and animals with the S21A mutation in GRK1 ($298 \pm 15 \mu\text{V}$, $n = 15$, $P < .05$) (Figure 5A, bottom traces). The dark-adapted photosensitivities (a-wave) were similar in the two mouse lines ($1.5 \pm 0.05 \text{ m}^2\text{cd}^{-1}\text{s}^{-1}$ vs $1.6 \pm 0.04 \text{ m}^2\text{cd}^{-1}\text{s}^{-1}$, $P < .05$). Mutant rods also transmitted their signaling to ON-bipolar cells normally, as demonstrated by the comparable ERG b-waves in wild-type and GRK1-S21A mice. These findings are consistent with the data obtained with transretinal recordings (Figure 4) and indicate the normal function of GRK1-S21A rods in dark-adapted conditions.

To determine the possible role of GRK1 phosphorylation in modulating dark adaptation, we briefly exposed the mice to bright light to bleach >90% of the rhodopsin. Immediately after bleaching, rods in both wild-type and GRK1-S21A mutants generated barely detectable ERG a-wave responses that were desensitized by almost 3 log units (Figure 5A; second traces from the bottom). Photoresponses in both lines then gradually recovered over the following period of dark adaptation (Figure 5A; top three traces). The recovery of the averaged maximal ERG a-wave amplitude to a saturating flash intensity (A_{max}) in control rods could be described by a single exponential function with a time constant of 14.0 ± 0.8 minutes ($n = 16$), and its level by 75 minutes after the bleach was ~81% of the pre-bleach value (Figure 5B, black symbols). Although mutant rods also demonstrated robust recovery from the bleach, the rate of dark adaptation (17.3 ± 0.9 minutes, $n = 15$) was decreased compared to that of control rods, and the maximal response amplitude 75 minutes after the bleach reached only ~69% of control rods in the dark (Figure 5B, red symbols). A similar suppression of dark adaptation was observed in the recovery of rod-driven ERG a-wave sensitivity (S_f , see Methods for definition) following the same bleach (Figure 5C).

Taken together, these results clearly demonstrate that the point mutation S21A in GRK1 causes a delay in the recovery of efficient rod signaling and rhodopsin regeneration after exposure to bright light. Thus, phosphorylation of GRK1 at this residue is important for timely dark adaptation of mouse rods. Although the final relative level of postbleach response recovery was ~12% lower in mutant mice, the slow trend in its rescue suggests that the photosensitivity would reach the same level as that in wild-type animals after overnight dark adaptation, as measured by transretinal ERG recordings (Figure 4C,D).

3.5 | Cone phototransduction and dark adaptation in GRK1-S21A mice

It has been established previously that unlike many other mammals which express both GRK1 and GRK7 in their cone photoreceptors, mouse cone cells solely express GRK1 (see Ref. 36 for review). To determine whether the S21A mutation in GRK1 also affects the phototransduction cascade in mouse cones and their signaling, we carried out *ex vivo* ERG

recordings from dark-adapted animals derived on the *Gnat1*^{-/-} background. The lack of the transducin α -subunit eliminates the rod component of the light response in these mice without affecting cone morphology or function.²⁷ Our analysis was limited to M cones, which can be selectively stimulated with visible green light.

Recordings from isolated retinas in the presence of postsynaptic blockers revealed that under dark-adapted conditions the flash responses of M-cones from GRK1-S21A mice had amplitudes (Figure 6A,B), kinetics (Figure 6C, and its inset showing saturated responses), and sensitivity (Figure 6D) comparable to those of M-cone responses from control animals. Thus, as in the case of rods, the S21A mutation in cone-expressed GRK1 did not affect the overall health or phototransduction in these photoreceptors. Surprisingly, however, ERG recordings from live animals showed that M-cone dark adaptation (estimated from the recovery of cone ERG b-wave flash sensitivity) after a near complete bleaching of cone visual pigment was essentially normal in the mutant mice (Figure 6E). These findings imply that, in contrast to the case in rods, GRK1-Ser21 phosphorylation/dephosphorylation does not modulate the resetting of M-cone pigment during cone dark adaptation.

4 | DISCUSSION

In the present report, we tested the hypothesis that modulation of GRK1 activity by reversible light/dark-dependent phosphorylation at Ser21 regulates the kinetics of recovery of mammalian retinal photoreceptors from exposure to bright light and is required for their timely dark adaptation in vivo. We generated mice in which alanine was substituted for the amino acid Ser21, the cAMP-dependent phosphorylation site in GRK1²¹ (Figure 1). Mutating GRK1 to block cAMP-dependent phosphorylation at Ser21 did not affect the expression levels of GRK1 or the G protein transducin in mouse rods (Figure 2) and did not cause detectable retinal degeneration up to 4 months of age (Figure 3). We then determined that dark-adapted GRK1-S21A mutant mice displayed similar rod photoresponses as their wild-type counterparts, as measured by transretinal ERG (Figure 4). In striking contrast, rod dark adaptation after a bleach activating approximately 90% of rhodopsin was significantly delayed in rods expressing the mutant GRK1 (Figure 5), indicating that phosphorylation at Ser21 in GRK1 in wild-type animals normally leads to faster recovery of the pigment's ground state. However, mutant rods appeared to gradually recover photosensitivity to their normal pre-bleach level in the absence of the phosphorylated form of GRK1. The presence of a fraction of phosphorylated rhodopsin would reduce the efficiency of subsequent activation of the phototransduction cascade³⁵ and lower the sensitivity of mouse rods.¹⁴ Therefore, the observed normal sensitivity in fully (overnight) dark-adapted mutant rods (Figure 4C) implies that pigment dephosphorylation by PP2A¹⁸ and regeneration are completed within several hours in the dark even in GRK1-S21A mutant rods. Quantitative time-resolved rhodopsin phosphorylation analysis is not trivial¹⁸ and future experiments will seek to confirm directly the effect of the S21A mutation of GRK1 on the kinetics and level of rhodopsin phosphorylation following exposure to bright light and during subsequent dark adaptation. However, our earlier experiments in vitro demonstrated that GRK1 phosphorylated at Ser21 slowed rhodopsin phosphorylation, which would be expected to lead to faster recovery of rod sensitivity in vivo, and the S21A mutant enhanced rhodopsin

phosphorylation,²¹ which would be predicted to slow the recovery. These results are consistent with our observations in the present study.

It should be noted that the amount of rhodopsin activated by a single, even saturating, test flash in our experiments is rather low (~0.001% of the total pigment content per average mouse rod). Therefore, both wild-type GRK1, whose level in mouse rods constitutes ~2%-3% of that of the entire rhodopsin content,³⁷ and the more active GRK1-S21A,²¹ whose amount is comparable to that in control cells (Figure 2), are expected to have sufficient capacity to phosphorylate photoactivated pigment under these conditions. Moreover, it is well established that rhodopsin phosphorylation is normally not the rate-limiting step in recovery of the photoresponse in mouse rods.³⁸ Thus, relatively moderate (less than 50%) differences in pigment phosphorylation rates in GRK1-S21A vs. phosphorylated wild-type GRK1²¹ are not expected to produce a significant effect on the time course of photoresponse inactivation, as confirmed by our results. This is in contrast to the situation when 3- to 12-fold overexpression of wild-type GRK1 significantly accelerated the recovery phase of both dim flash and saturated responses in mouse rods.^{39,40} Overall, these findings are consistent with the emerging evidence that the GRK1-dependent modulation of rhodopsin's lifetime and/or phosphodiesterase activity becomes noticeable only at certain levels or activity of the enzyme in mouse photoreceptors. Although this modulation does not affect the function of rods in dark-adapted conditions, it becomes significant after exposure to bright bleaching light during the subsequent pigment regeneration and dark adaptation. As a result, the GRK-dependent modulation of rhodopsin appears as a mechanism that accelerates the recycling of the pigment and the dark adaptation of rod photoreceptors.

Cyclic AMP-dependent phosphorylation of wild-type GRK1 in the dark is comparatively slow, taking on the order of 10-20 minutes to approach 80% completion *in vivo*.²⁵ Therefore, the ability of wild-type GRK1 to phosphorylate rhodopsin may be decreasing progressively over the recovery time course as GRK1 is slowly phosphorylated, thereby reducing its activity and increasing the ability of rods to dark-adapt after extensive bleaching of their visual pigment (Figure 5). The mechanism by which phosphorylation at Ser21 in GRK1 increases phosphorylation of rhodopsin is unknown. However, it is interesting to note that the first 19 amino acids of GRK1, which are disordered and therefore not visible in the crystal structure, are proposed to form an α -helix that interacts with and stabilizes the kinase domain in the presence of rhodopsin.^{41,42} Crosslinking studies suggested that the amino-terminal domain is important for activation of GRK1.⁴³ Therefore, it is possible that phosphorylation at Ser21 affects the stability, and therefore the level of activity, of the kinase domain. One important future line of investigation is the mechanism by which GRK1 is dephosphorylated in the presence of light, specifically the enzyme responsible for this reaction and the mechanism of its modulation by light.

Interestingly, our previous work demonstrated that elevated phosphorylation of rhodopsin in the absence of the major catalytic subunit of protein phosphatase 2A (PP2A) resulted in a reduced rate of dark adaptation after a full rhodopsin bleach in intact mouse eyes.¹⁸ The time constant for recovery of the scotopic ERG a-wave during dark adaptation was nearly twofold larger in PP2A-C α -deficient mice compared to controls,¹⁸ indicating a 50%

decrease in the rate of rod responsiveness during recovery. In our present study, performed on animals with a somewhat different genetic background, the time constant for recovery of the scotopic ERG a-wave for the GRK1-S21A mice during dark adaptation following a similar pigment bleach was 17.3 ± 0.9 minutes compared to 14.0 ± 0.8 minutes for the wild-type animals, indicating a 24% decrease in the rate of rod dark adaptation. The approximately two times smaller difference in the recovery time constant between the control and GRK1-S21A mice in the current report suggests that the presence of PP2A may partially negate the effect of the more active kinase in the GRK1-S21A mice and strengthens the hypothesis that the phosphorylation status of rhodopsin plays an important role in photoreceptor dark adaptation. In support of this idea, a recent study demonstrated that the lack of rhodopsin phosphorylation in GRK1-deficient mouse rods moderately accelerated the thermal decay of the long-lived, inactive rhodopsin photoproduct, Meta III, and speeded up the regeneration of free opsin with exogenous 11-*cis*-retinal.¹⁶ Furthermore, the same study reported faster dark adaptation in rods of *Grk1*^{+/-} mice, which express GRK1 at ~30% of wild-type levels. Together, these findings strongly suggest that the reduced rate of the recovery of the dark pigment state in GRK1-S21A mice may be due to slower chromophore release from the hyperphosphorylated bleached photopigment, thus suppressing the recycling of opsin back to rhodopsin by regeneration with 11-*cis*-retinal in the final step of the RPE-driven visual cycle.

Finally, it is well known that the visual pigment regeneration and dark adaptation of human, mouse, and other mammalian species' cones proceeds with substantially faster kinetics than that in their rod counterparts (reviewed in 13). It has been established that the combined action of the RPE and intraretinal (Müller cell-driven) visual cycles is required for the rapid and complete dark adaptation of vertebrate cones *in vivo*.⁴⁴ Furthermore, our recent work has demonstrated that, as in mouse rods, dephosphorylation of opsin by PP2A after exposure to intense bleaching light controls the process of dark adaptation of M-cone photoreceptors as well.¹⁸ Because the biochemical characterization of the regulation of cone dark adaptation is currently unfeasible due to the scarcity of cones in the mouse retina,⁴⁵ we applied the same physiological approaches to address the question of whether a similar regulatory mechanism through phosphorylation at Ser21 in GRK1 potentially exists in these cells. Using transretinal ERG recordings, we found that, as in the case of rods, dark-adapted GRK1-S21A mutant mice had cone photoresponses identical to those in their respective control animals (Figure 6A-D). Surprisingly, however, M-cone dark adaptation after a nearly complete pigment bleach was unaffected by the GRK1 mutation (Figure 6E), thus indicating that phosphorylation at Ser21 in GRK1 is not essential for the rapid recovery of at least this type of cone pigment's ground state in mice.

For convenience, all our cone recordings were performed with mice lacking the rod transducin α -subunit (*Gnat1*^{-/-}), which allows for isolation of the cone photoresponse. As this subunit is not found in cones, and cone phototransduction appears to be normal,³⁴ it is unlikely that its absence would influence cone function, including cone pigment dephosphorylation and cone adaptation. Notably, using this method Kolesnikov et al found that the deletion of PP2A in cones delays their dark adaptation similarly to the effect in rods.¹⁸ Although we cannot absolutely rule out the possibility that a signal transmitted via gap

junctions between rods and cones could influence cone dark adaptation via GRK1 in the *Gnat1*^{-/-} mice, we have no evidence to propose such a hypothesis.

The reason for the lack of GRK1 phosphorylation-dependent regulation of visual pigment recycling in cone photoreceptors is unclear. It has been shown that GRK1 is necessary for timely inactivation of phototransduction in mouse cones⁴⁶ and it might be present at higher levels in these cells, as compared to rods.⁸ However, cones could also potentially express a higher compensatory amount of total PP2A and/or other opsin phosphatases than rods. Notably, it has been demonstrated previously that the dephosphorylation of cone opsin in vertebrates proceeds significantly faster than that of rhodopsin.^{47,48} Furthermore, a very rapid thermal decay of photoactivated cone pigment^{49,50} would quickly reduce the efficiency of its subsequent interactions with GRK1 within the first several seconds of dark adaptation and thus minimize the overall effect of kinase activity on the following cone opsin regeneration with 11-*cis*-retinal. These are important issues for further investigation.

In summary, our results demonstrate a role for cAMP-dependent phosphorylation of GRK1 in modulating the kinetics of rod dark adaptation in the mammalian retina. Although rod and cone response recovery after dim and saturating flashes was similar between GRK1-S21A and control animals, the dark adaptation of rods (but not M-cones) following exposure to bright light was significantly delayed in the mutant mice due to the presence of a more active kinase. Similar to the results from studies in PP2A deletion mice,¹⁸ phosphorylation at Ser21 in GRK1 appears to play an important role in the recovery of the dark state of the photopigment in rod photoreceptors.

ACKNOWLEDGMENTS

The authors would like to thank the Animal Models Core at UNC-Chapel Hill for the generation of the GRK1-S21A mice, Dr Ching-Kang Chen for the *Grk1*^{-/-} mice and the Duke University Eye Center Core for assistance with retina preparation and analysis. This work was supported by NIH grants EY01224 (ERW), EY026675 and EY019312 (VJK), the NEI Core Grants for Vision Research at Duke University (EY05722; ERW) and at Washington University (EY02687; VJK), and by Research to Prevent Blindness (VJK). We would also like to thank Dr. Marie Burns from the University of California Davis for helpful discussions.

Funding information

HHS | NIH | National Eye Institute (NEI), Grant/Award Number: EY01224, EY005722 (Duke Univ. Core), EY026675, EY019312 and EY02687 (Washington Univ. Core); Research to Prevent Blindness (RPB)

Abbreviations:

BAC	bacterial artificial chromosome
cAMP	cyclic AMP
ERG	electroretinography
GCL	ganglion cell layer
GPCR	G protein-coupled receptor
GRK1	G protein-coupled receptor kinase 1

GRK7	G protein-coupled receptor kinase 7
INL	inner nuclear layer
IS	inner segments
LED	light-emitting diode
ONH	optic nerve head
ONL	outer nuclear layer
OS	outer segments
PDE6	phosphodiesterase 6
PP2A	protein phosphatase 2A
pGRK1	GRK1 phosphorylated on Serine 21
RPE	retinal pigment epithelium
SEM	standard error of the mean

REFERENCES

1. Arshavsky VY, Burns ME. Photoreceptor signaling: supporting vision across a wide range of light intensities. *J Biol Chem.* 2012;287:1620–1626. [PubMed: 22074925]
2. Latek D, Modzelewska A, Trzaskowski B, Palczewski K, Filipek S. G protein-coupled receptors—recent advances. *Acta Biochim Pol.* 2012;59:515–529. [PubMed: 23251911]
3. Weiss ER, Ducceschi MH, Horner TJ, Li A, Craft CM, Osawa S. Species-specific differences in expression of G-protein-coupled receptor kinase (GRK) 7 and GRK1 in mammalian cone photoreceptor cells: implications for cone cell phototransduction. *J Neurosci.* 2001;21:9175–9184. [PubMed: 11717351]
4. Wada Y, Sugiyama J, Okano T, Fukada Y. GRK1 and GRK7: unique cellular distribution and widely different activities of opsin phosphorylation in the zebrafish rods and cones. *J Neurochem.* 2006;98:824–837. [PubMed: 16787417]
5. Tachibanaki S, Arinobu D, Shimauchi-Matsukawa Y, Tsushima S, Kawamura S. Highly effective phosphorylation by G protein-coupled receptor kinase 7 of light-activated visual pigment in cones. *Proc Natl Acad Sci U S A.* 2005;102:9329–9334. [PubMed: 15958532]
6. Schott RK, Van Nynatten A, Card DC, Castoe TA, Chang BSW. Shifts in selective pressures on snake phototransduction genes associated with photoreceptor transmutation and dim-light ancestry. *Mol Biol Evol.* 2018;35:1376–1389. [PubMed: 29800394]
7. Zhao XY, Huang J, Khani SC, Palczewski K. Molecular forms of human rhodopsin kinase (GRK1). *J Biol Chem.* 1998;273:5124–5131. [PubMed: 9478965]
8. Maeda T, Imanishi Y, Palczewski K. Rhodopsin phosphorylation: 30 years later. *Prog Ret Eye Res.* 2003;22:417–434.
9. Gurevich VV, Hanson SM, Song X, Vishnivetskiy SA, Gurevich EV. The functional cycle of visual arrestins in photoreceptor cells. *Prog Retin Eye Res.* 2011;30:405–430. [PubMed: 21824527]
10. Makino CL, Wen XH, Lem J. Piecing together the timetable for visual transduction with transgenic animals. *Curr Opin Neurobiol.* 2003;13:404–412. [PubMed: 12965286]
11. Makino CL, Dodd RL, Chen J, et al. Recoverin regulates light-dependent phosphodiesterase activity in retinal rods. *J Gen Physiol.* 2004;123:729–741. [PubMed: 15173221]
12. Sakurai K, Chen J, Khani SC, Kefalov VJ. Regulation of mammalian cone phototransduction by recoverin and rhodopsin kinase. *J Biol Chem.* 2015;290:9239–9250. [PubMed: 25673692]

13. Lamb TD, Pugh EN Jr., Dark adaptation and the retinoid cycle of vision. *Prog Retin Eye Res.* 2004;23:307–380. [PubMed: 15177205]
14. Berry J, Frederiksen R, Yao Y, Nymark S, Chen J, Cornwall C. Effect of rhodopsin phosphorylation on dark adaptation in mouse rods. *J Neurosci.* 2016;36:6973–6987. [PubMed: 27358455]
15. Lee KA, Nawrot M, Garwin GG, Saari JC, Hurley JB. Relationships among visual cycle retinoids, rhodopsin phosphorylation, and phototransduction in mouse eyes during light and dark adaptation. *Biochemistry.* 2010;49:2454–2463. [PubMed: 20155952]
16. Frederiksen R, Nymark S, Kolesnikov AV, et al. Rhodopsin kinase and arrestin binding control the decay of photoactivated rhodopsin and dark adaptation of mouse rods. *J Gen Physiol.* 2016;148:1–11. [PubMed: 27353443]
17. Mata NL, Radu RA, Clemmons RC, Travis GH. Isomerization and oxidation of vitamin a in cone-dominant retinas: a novel pathway for visual-pigment regeneration in daylight. *Neuron.* 2002;36:69–80. [PubMed: 12367507]
18. Kolesnikov AV, Orban T, Jin H, et al. Dephosphorylation by protein phosphatase 2A regulates visual pigment regeneration and the dark adaptation of mammalian photoreceptors. *Proc Natl Acad Sci U S A.* 2017;114:E9675–E9684. [PubMed: 29078372]
19. Hisatomi O, Matsuda S, Satoh T, Kotaka S, Imanishi Y, Tokunaga F. A novel subtype of G-protein-coupled receptor kinase, GRK7, in teleost cone photoreceptors. *FEBS Lett.* 1998;424:159–164. [PubMed: 9539142]
20. Weiss ER, Raman D, Shirakawa S, et al. The cloning of GRK7, a candidate cone opsin kinase, from cone- and rod-dominant mammalian retinas. *Mol Vis.* 1998;4:27 <http://www.molvis.org/molvis/v4/p27>. [PubMed: 9852166]
21. Horner TJ, Osawa S, Schaller MD, Weiss ER. Phosphorylation of GRK1 and GRK7 by cAMP-dependent protein kinase attenuates their enzymatic activities. *J Biol Chem.* 2005;280: 28241–28250. [PubMed: 15946941]
22. Cohen AI, Blazynski C. Dopamine and its agonists reduce a light-sensitive pool of cyclic AMP in mouse photoreceptors. *Visual Neurosci.* 1990;4:43–52.
23. Farber DB, Souza DW, Chase DG, Lolley RN. Cyclic nucleotides of cone-dominant retinas. Reduction of cyclic AMP levels by light and by cone degeneration. *Invest Ophthalmol Vis Sci.* 1981;20:24–31. [PubMed: 6256308]
24. Osawa S, Jo R, Weiss ER. Phosphorylation of GRK7 by PKA in cone photoreceptor cells is regulated by light. *J Neurochem.* 2008;107:1314–1324. [PubMed: 18803695]
25. Osawa S, Jo R, Xiong Y, et al. Phosphorylation of G protein-coupled receptor kinase 1 (GRK1) is regulated by light but independent of phototransduction in rod photoreceptors. *J Biol Chem.* 2011;286:20923–20929. [PubMed: 21504899]
26. Caenepeel S, Charydczak G, Sudarsanam S, Hunter T, Manning G. The mouse kinome: discovery and comparative genomics of all mouse protein kinases. *Proc Natl Acad Sci U S A.* 2004;101:11707–11712. [PubMed: 15289607]
27. Calvert PD, Krasnoperova NV, Lyubarsky AL, et al. Phototransduction in transgenic mice after targeted deletion of the rod transducin alpha -subunit. *Proc Natl Acad Sci U S A.* 2000;97:13913–13918. [PubMed: 11095744]
28. Lee BY, Thulin CD, Willardson BM. Site-specific phosphorylation of phosducin in intact retina. Dynamics of phosphorylation and effects on G protein $\beta\gamma$ dimer binding. *J Biol Chem.* 2004;279:54008–54017. [PubMed: 15485848]
29. Schneider CA, Rasband WS, Eliceiri KW. NIH Image to ImageJ: 25 years of image analysis. *Nat Methods.* 2012;9:671–675. [PubMed: 22930834]
30. Vinberg F, Kolesnikov AV, Kefalov VJ. Ex vivo ERG analysis of photoreceptors using an in vivo ERG system. *Vision Res.* 2014;101:108–117. [PubMed: 24959652]
31. Sillman AJ, Ito H, Tomita T. Studies on the mass receptor potential of the isolated frog retina. I. General properties of the response. *Vision Res.* 1969;9:1435–1442. [PubMed: 5367433]
32. Nymark S, Heikkinen H, Haldin C, Donner K, Koskelainen A. Light responses and light adaptation in rat retinal rods at different temperatures. *J Physiol.* 2005;567:923–938. [PubMed: 16037091]

33. Woodruff ML, Lem J, Fain GL. Early receptor current of wild-type and transducin knockout mice: photosensitivity and light-induced Ca²⁺ release. *J Physiol*. 2004;557:821–828. [PubMed: 15073279]
34. Nikonov SS, Kholodenko R, Lem J, Pugh EN Jr., Physiological features of the S- and M-cone photoreceptors of wild-type mice from single-cell recordings. *J Gen Physiol*. 2006;127:359–374. [PubMed: 16567464]
35. Gibson SK, Parkes JH, Liebman PA. Phosphorylation modulates the affinity of light-activated rhodopsin for G protein and arrestin. *Biochemistry*. 2000;39:5738–5749. [PubMed: 10801324]
36. Osawa S, Weiss ER. A tale of two kinases in rods and cones. *Adv Exp Med Biol*. 2012;723:821–827. [PubMed: 22183412]
37. Chen C-K, Woodruff ML, Chen FS, et al. Modulation of mouse rod response decay by rhodopsin kinase and recoverin. *J Neurosci*. 2012;32:15998–16006. [PubMed: 23136436]
38. Krispel CM, Chen D, Melling N, et al. RGS expression rate-limits recovery of rod photoresponses. *Neuron*. 2006;51:409–416. [PubMed: 16908407]
39. Chen CK, Woodruff ML, Fain GL. Rhodopsin kinase and recoverin modulate phosphodiesterase during mouse photoreceptor light adaptation. *J Gen Physiol*. 2015;145:213–224. [PubMed: 25667411]
40. Sakurai K, Young JE, Kefalov VJ, Khani SC. Variation in rhodopsin kinase expression alters the dim flash response shut off and the light adaptation in rod photoreceptors. *Invest Ophthalmol Vis Sci*. 2011;52:6793–6800. [PubMed: 21474765]
41. Orban T, Huang CC, Homan KT, Jastrzebska B, Tesmer JJ, Palczewski K. Substrate-induced changes in the dynamics of rhodopsin kinase (G protein-coupled receptor kinase 1). *Biochemistry*. 2012;51:3404–3411. [PubMed: 22480180]
42. Singh P, Wang B, Maeda T, Palczewski K, Tesmer JJ. Structures of rhodopsin kinase in different ligand states reveal key elements involved in G protein-coupled receptor kinase activation. *J Biol Chem*. 2008;283:14053–14062. [PubMed: 18339619]
43. Huang CC, Orban T, Jastrzebska B, Palczewski K, Tesmer JJ. Activation of G protein-coupled receptor kinase 1 involves interactions between its N-terminal region and its kinase domain. *Biochemistry*. 2011;50:1940–1949. [PubMed: 21265573]
44. Kolesnikov AV, Tang PH, Parker RO, Crouch RK, Kefalov VJ. The mammalian cone visual cycle promotes rapid M/L-cone pigment regeneration independently of the interphotoreceptor retinoid-binding protein. *J Neurosci*. 2011;31:7900–7909. [PubMed: 21613504]
45. Carter-Dawson LD, LaVail MM. Rods and cones in the mouse retina. I. Structural analysis using light and electron microscopy. *J Comp Neurol*. 1979;188:245–262. [PubMed: 500858]
46. Lyubarsky AL, Chen C-K, Simon MI, Pugh EN. Mice lacking G-protein receptor kinase 1 have profoundly slowed recovery of cone-driven retinal responses. *J Neurosci*. 2000;20:2209–2217. [PubMed: 10704496]
47. Kennedy MJ, Dunn FA, Hurley JB. Visual pigment phosphorylation but not transducin translocation can contribute to light adaptation in zebrafish cones. *Neuron*. 2004;41:915–928. [PubMed: 15046724]
48. Yamaoka H, Tachibanaki S, Kawamura S. Dephosphorylation during bleach and regeneration of visual pigment in carp rod and cone membranes. *J Biol Chem*. 2015;290:24381–24390. [PubMed: 26286749]
49. Ala-Laurila P, Kolesnikov AV, Crouch RK, et al. Visual cycle: dependence of retinol production and removal on photoproduct decay and cell morphology. *J Gen Physiol*. 2006;128:153–169. [PubMed: 16847097]
50. Imai H, Terakita A, Tachibanaki S, Imamoto Y, Yoshizawa T, Shichida Y. Photochemical and biochemical properties of chicken blue-sensitive cone visual pigment. *Biochemistry*. 1997;36:12773–12779. [PubMed: 9335534]

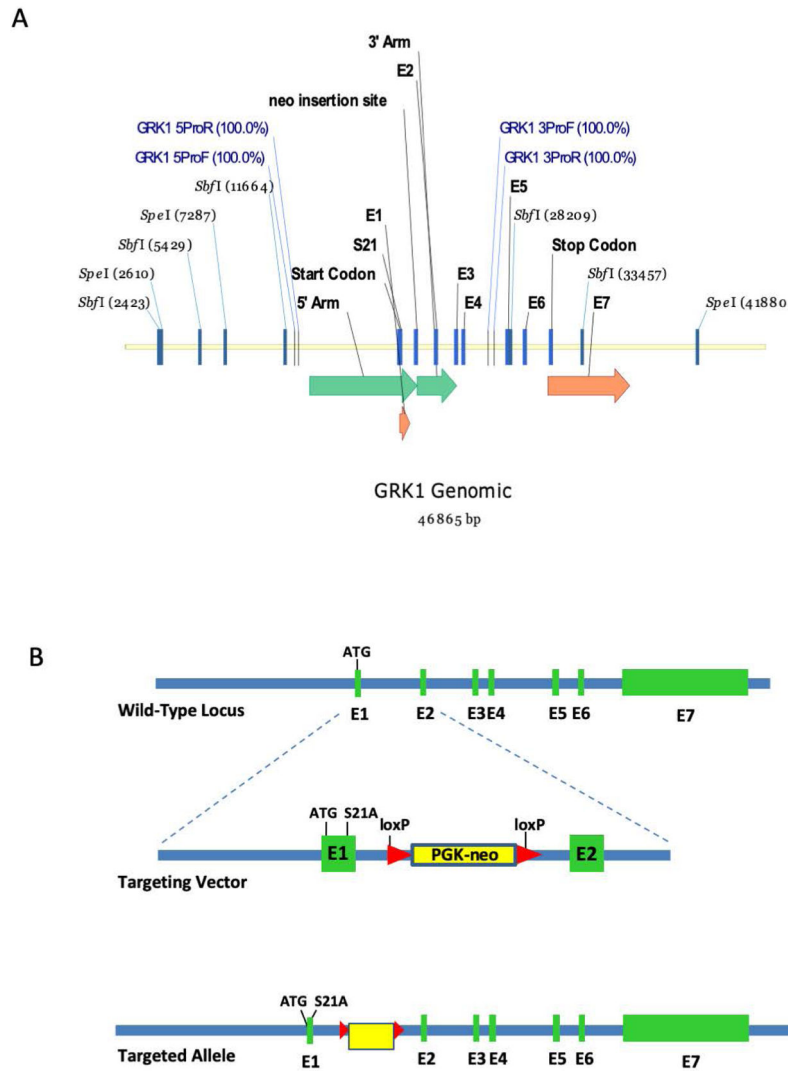
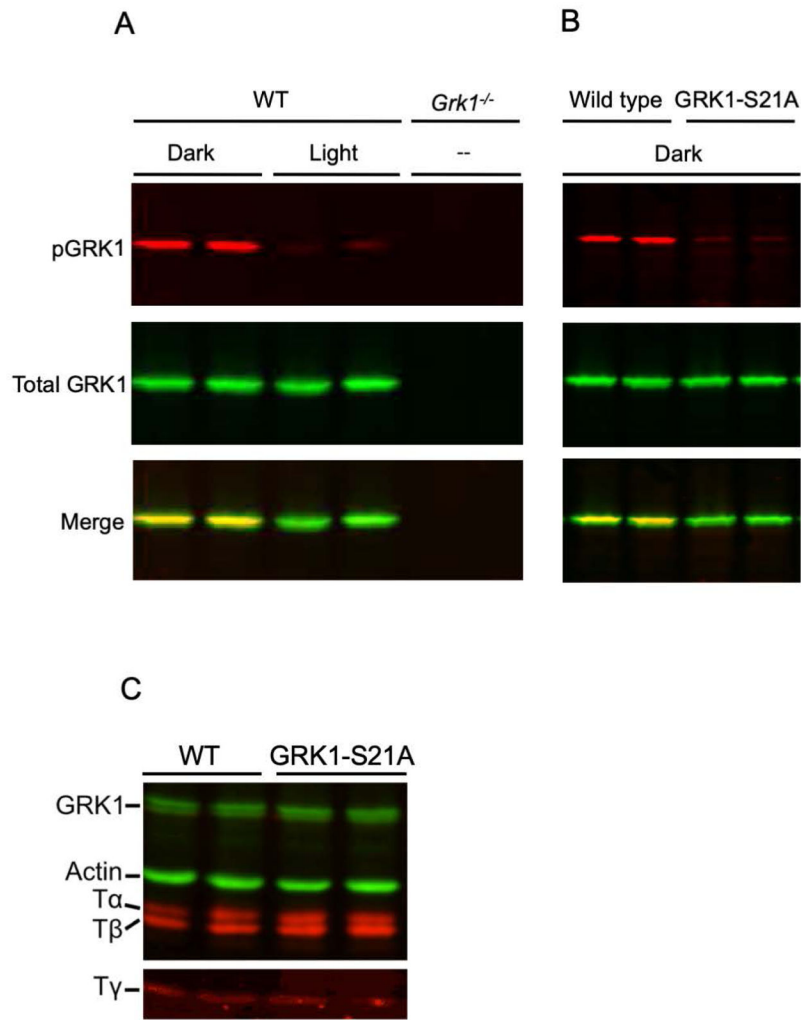


FIGURE 1. Strategy for generation of the GRK1-S21A mutant mouse. A, Genomic clone of wild-type *Grk1*. Green arrows represent areas covered by the vector homology arms (long arrow is the 5' arm, short arrow is the 3' arm). Orange arrows indicate the positions of exons 1 and 7, respectively. The other exons are represented by blue bars. B, Generation of the mutant S21A-GRK1 allele. The wild-type locus is shown on top. An expanded view of the first two exons is shown in the middle containing the Ser21Ala (S21A) mutation and a PKG-neo cassette with *loxP* sites on either end. The lower panel shows the entire targeted allele with the S21A mutation, the PKG-neo cassette and the 7 exons

**FIGURE 2.**

Characterization of the GRK1-S21A mouse. A, Western blot analysis of retinas from 4- to 5-month-old wild-type and GRK1 knockout (*Grk1^{-/-}*) mice. Wild-type mice raised in cyclic light were dark-adapted overnight, then either exposed to 1500-lux light for 1 hour or and maintained in the dark. The light-exposed mice were euthanized in the light and the mice maintained in the dark were euthanized under dim red light and their retinas removed for western blot analysis. *Grk1^{-/-}* mice were raised in the dark and retinas prepared under infrared light. The blot was incubated with anti-pGRK1 (red) or anti-GRK1 (green) antibodies. These data were originally published in the Journal of Biological Chemistry ©The American Society for Biochemistry and Molecular Biology (Ref. 25). B, Western blot analysis of retinas from 4- to 5-month-old control and GRK1-S21A mice. Mice were dark-adapted overnight, euthanized in the dark and retinas removed for Western blot analysis. The blot was incubated with anti-pGRK1 (red) and anti-GRK1 (green) antibodies. C, Western blot analysis was performed on retinas from 4- to 5-month-old wild-type and GRK1-S21A mice using a polyclonal antibody that recognizes all three subunits of rod transducin (red), anti-pGRK1 (green), and a monoclonal antibody directed against actin (green)

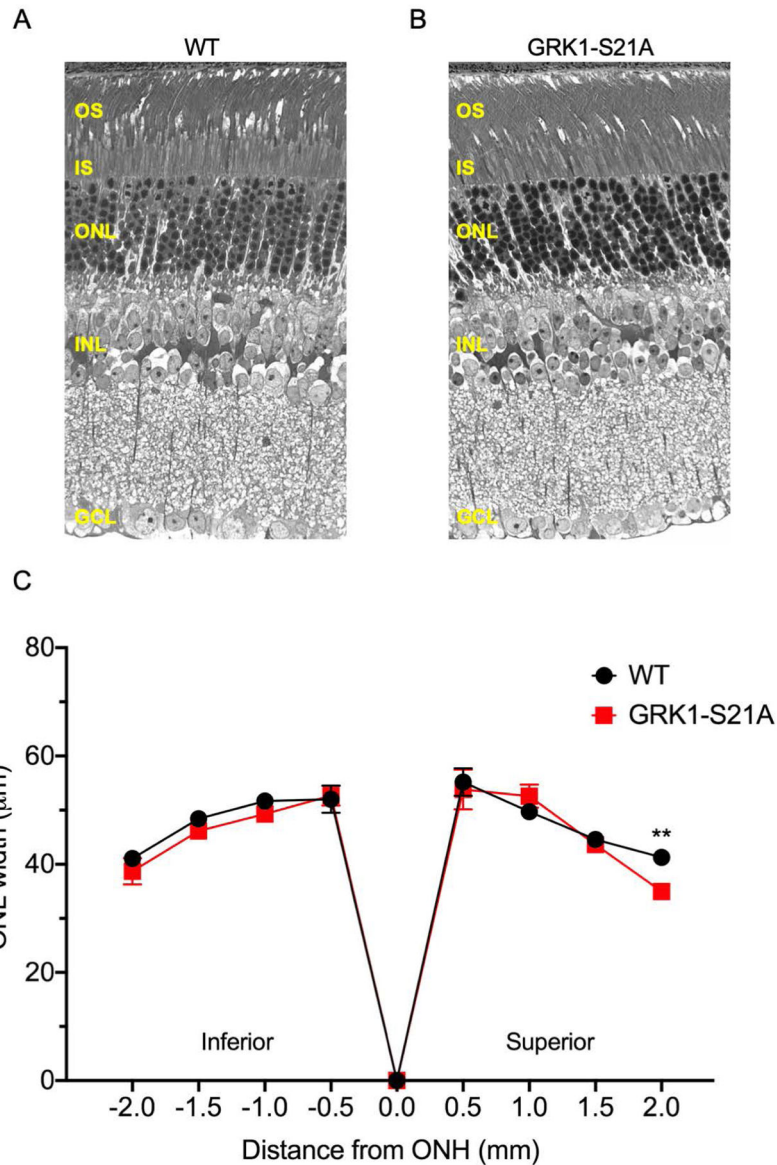
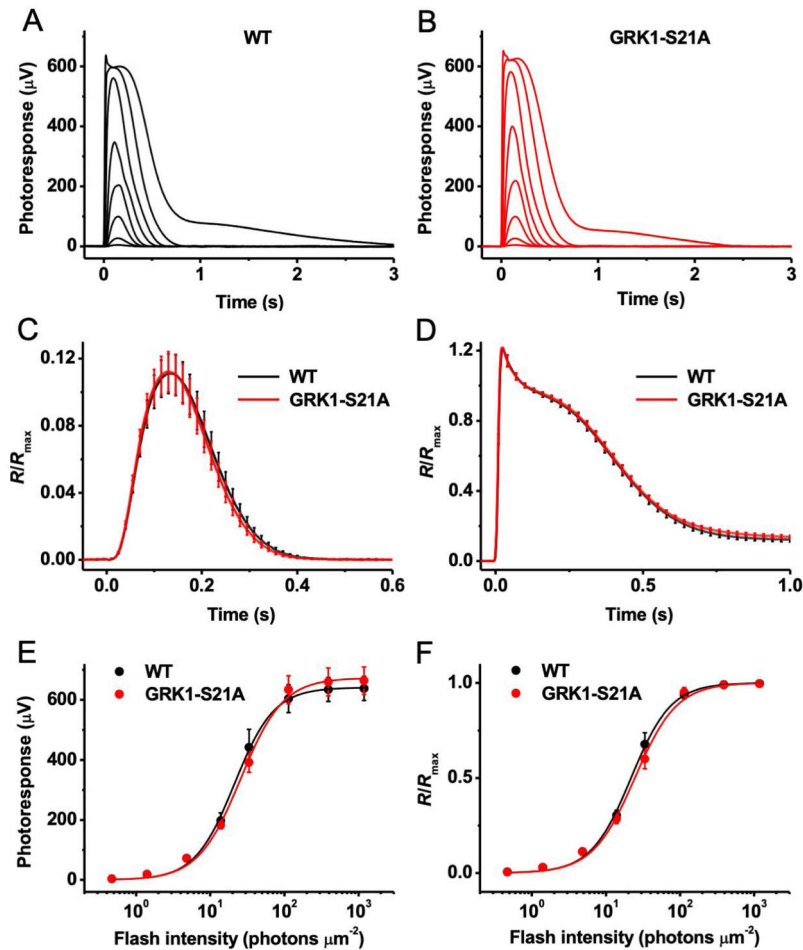
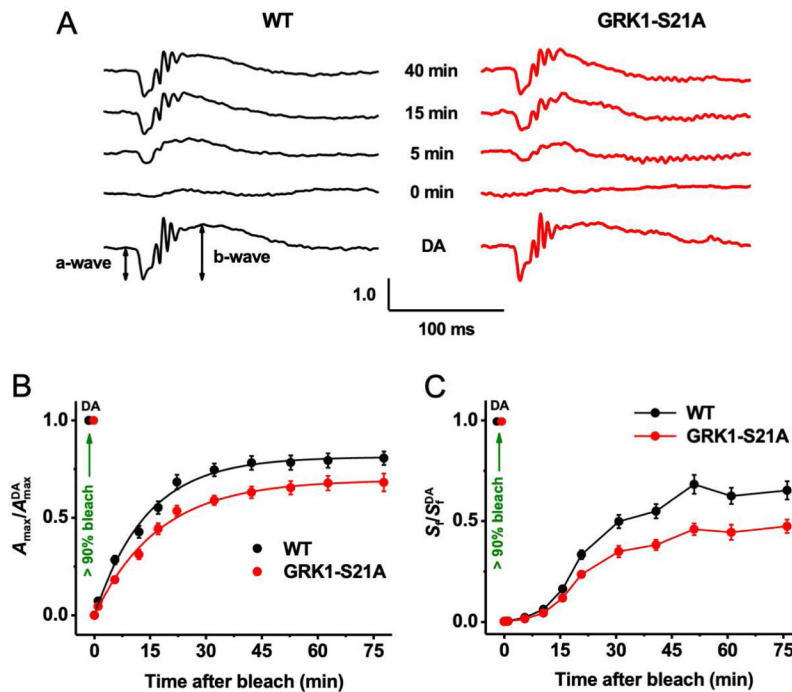


FIGURE 3.

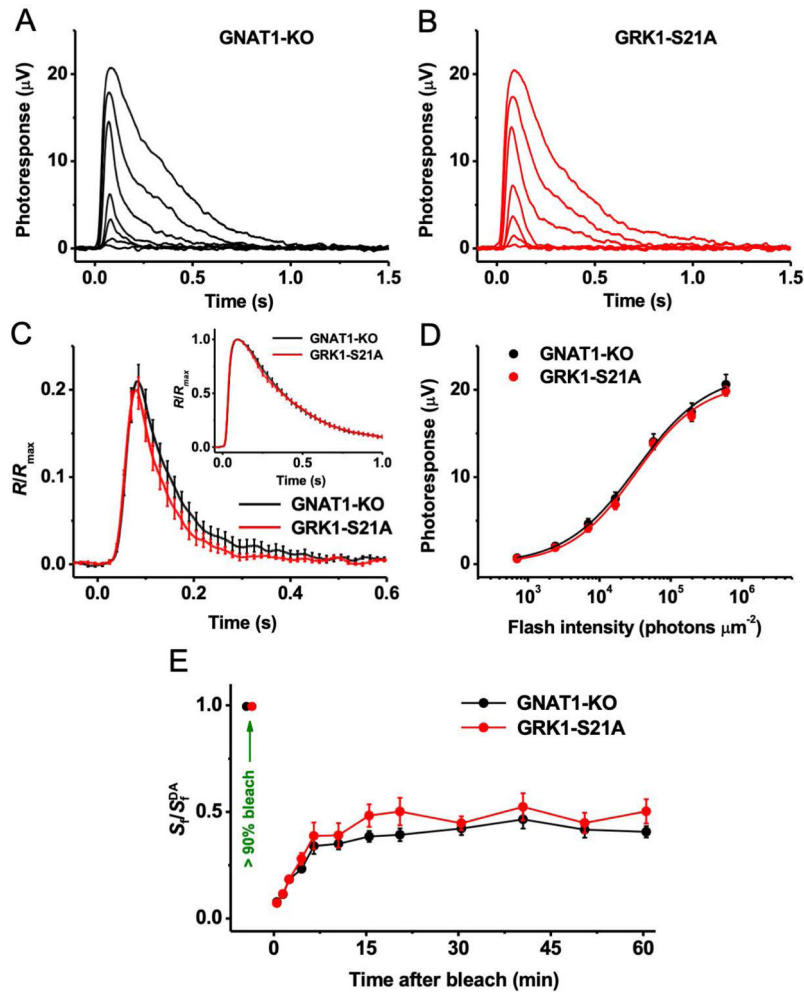
Comparison of the outer nuclear layer (ONL) width in 4-month-old wild-type and GRK1-S21A mice. Eyes were enucleated, fixed, and sectioned as described in the Methods section. Microscopy images from control (A) and GRK-S21A mouse (B) retinas were compared and found to be very similar. C, The width of the ONL was measured at 500 µm intervals from the optic nerve head (ONH). No differences were identified except at the superior edge of the section, where there was a small but significant difference between wild-type and GRK1-S21A mice. ** $P < .01$ ($n = 6$ for each genotype; error bars represent SEM). GCL, ganglion cell layer; INL, inner nuclear layer; IS, inner segments; OS, outer segments

**FIGURE 4.**

Ex vivo rod ERG responses of wild-type and GRK1-S21A mice. A, Representative family of rod responses from wild-type mouse retina. Test flashes of 505 nm light with intensities of 0.5, 1.4, 4.8, 14, 33, 114, 392, and 1188 photons μm^{-2} were delivered at time 0. B, Representative family of rod responses from GRK1-S21A mouse retina. Test flashes of 505 nm light had the same intensities as in A. C, Kinetics of rod phototransduction activation and inactivation in control and GRK1-S21A mice. Population-averaged (mean \pm SEM) dim flash responses to test stimuli of 4.8 photons μm^{-2} ($n = 10$ for each line) were normalized to maximal response amplitudes (R_{max}) of respective retinas. D, Comparison of saturated rod responses from WT and GRK1-S21A animals. Population-averaged (mean \pm SEM) responses to test stimuli of 1188 photons μm^{-2} ($n = 10$ for each strain) were normalized to R_{max} of respective retinas. E, Averaged rod intensity-response functions (mean \pm SEM) for wild-type ($n = 10$) and GRK1-S21A ($n = 10$) retinas. Points were fitted with hyperbolic Naka-Rushton functions (see Methods). F, Normalized averaged rod intensity-response relationships (mean \pm SEM) for wild-type ($n = 10$) and GRK1-S21A ($n = 10$) retinas. Naka-Rushton fits yielded half-saturating intensities ($I_{1/2}$) of 22 and 24 photons μm^{-2} for wild-type and GRK1-S21A animals, respectively

**FIGURE 5.**

Suppressed rod dark adaptation in GRK1-S21A mice. **A**, Representative scotopic ERG responses in the dark (dark-adapted [DA], bottom) and at four indicated time points after bleaching >90% of the rod pigment in wild-type (left) and GRK1-S21A (right) mice. For each time point, A_{max} values were normalized to their corresponding pre-bleach dark-adapted value (A_{max}^{DA}). **B**, Recovery of scotopic ERG maximal a-wave amplitudes (A_{max} ; mean \pm SEM) after bleaching >90% of rhodopsin in wild-type ($n = 16$) and GRK1-S21A ($n = 15$) mice. Bleaching was achieved by a 35-s illumination with bright 520-nm LED light at time 0. Averaged data points were fitted with single exponential functions yielding time constants of 14.0 ± 0.8 and 17.3 ± 0.9 minutes for wild-type and S21A-GRK1 mice, respectively. Final levels of response recovery by 75 minutes postbleach determined from exponential fits were 81% (wild-type) and 69% (GRK1-S21A). **(C)** Recovery of scotopic ERG a-wave flash sensitivity (S_f ; mean \pm SEM) after bleaching >90% of rod pigment in wild-type ($n = 16$) and GRK1-S21A ($n = 15$) mice. S_f^{DA} designates the sensitivity of dark-adapted rods. Animals and experimental conditions were the same as in **B**

**FIGURE 6.**

Physiological characterization of M cones in control and GRK1-S21A mice and their dark adaptation. A, Representative family of cone responses from control (GRK1-WT-*Gnat1*^{-/-}) mouse retina. Test flashes of 505 nm light with intensities of 705, 2.4×10^3 , 7.0×10^3 , 1.7×10^4 , 5.7×10^4 , 2.0×10^5 , and 6.0×10^5 photons μm^{-2} were delivered at time 0. B, Representative family of cone responses from GRK1-S21A-*Gnat1*^{-/-} mouse retina. Test flashes of 505 nm light had the same intensities as in A. C, Kinetics of cone phototransduction in control and GRK1-S21A mice. Population-averaged (mean \pm SEM) dim flash responses to test stimuli of 7.0×10^3 photons μm^{-2} ($n = 11$ for each line) were normalized to maximal response amplitudes (R_{max}) of respective retinas. The inset shows the comparison of saturated cone responses from control and GRK1-S21A animals. Population-averaged (mean \pm SEM) responses to test stimuli of 6.0×10^5 photons μm^{-2} ($n = 11$ for each strain) were normalized to R_{max} of respective retinas. D, Averaged cone intensity-response functions (mean \pm SEM) for control and GRK1-S21A ($n = 11$ for each line) retinas. Naka-Rushton fits yielded half-saturating intensities ($I_{1/2}$) of 3.3×10^4 and 3.2×10^4 photons μm^{-2} for control and GRK1-S21A animals, respectively. E, Recovery of photopic ERG b-wave flash sensitivity (S_i ; mean \pm SEM) in vivo in control ($n = 20$) and GRK1-S21A ($n = 16$) mice after bleaching >90% of cone pigment at time 0 with 520 nm

LED light. S_f^{DA} designates the sensitivity of dark-adapted cones. At all times, there was no statistical significance of the data between control and mutant mice ($P > .05$)

Author Manuscript

Author Manuscript

Author Manuscript

Author Manuscript